



HAL
open science

Development of a multi-layering protein grafting process on miniaturized monolithic columns for weak affinity nano liquid chromatography application purposes

Andrea Gottardini, Vincent Dugas, Claire Demesmay

► To cite this version:

Andrea Gottardini, Vincent Dugas, Claire Demesmay. Development of a multi-layering protein grafting process on miniaturized monolithic columns for weak affinity nano liquid chromatography application purposes. *Journal of Chromatography A*, 2021, 1657, pp.462567. 10.1016/j.chroma.2021.462567 . hal-03508515

HAL Id: hal-03508515

<https://hal.science/hal-03508515v1>

Submitted on 16 Oct 2023

HAL is a multi-disciplinary open access archive for the deposit and dissemination of scientific research documents, whether they are published or not. The documents may come from teaching and research institutions in France or abroad, or from public or private research centers.

L'archive ouverte pluridisciplinaire **HAL**, est destinée au dépôt et à la diffusion de documents scientifiques de niveau recherche, publiés ou non, émanant des établissements d'enseignement et de recherche français ou étrangers, des laboratoires publics ou privés.



Distributed under a Creative Commons Attribution - NonCommercial 4.0 International License

1 **Development of a multi-layering protein grafting process on miniaturized monolithic columns for**
2 **weak affinity nano liquid chromatography application purposes**

3

4 Andrea Gottardini, Vincent Dugas, Claire Demesmay*

5

6 *Université de Lyon, CNRS, Université Claude Bernard Lyon 1, Institut des Sciences Analytiques, UMR 5280, 5 rue*
7 *de la Doua, F-69100 VILLEURBANNE, France*

8

9 * Corresponding author. Tel.: +33437423552

10 E-mail address: claire.demesmay@univ-lyon1.fr

11

12

13 **Abstract**

14 Affinity chromatography is a powerful technique to identify and quantify weak ligand-protein
15 interactions (K_d in the range of mM to 0.1 μ M). In some fields such as Fragment Based Drug
16 Discovery, the detection of very weak affinities (mM) is of utmost importance since weak ligands can
17 be good starting points for the conception of high affinity ligands. However, the identification of such
18 weak ligands can be hampered by the limited bulk density of active target grafted onto the support.
19 At the same time, downscaling the chromatographic column is of utmost interest when scarce
20 and/or expensive proteins are targeted. In this context, we herein present a novel approach of
21 protein immobilization to improve the bulk density of active protein grafted onto organic capillary
22 monolithic columns. The proposed approach is based on the streptavidin-biotin interaction and
23 consists of successive grafting steps of biotinylated target protein onto streptavidin layers through a
24 multi-layering process. Concanavalin A was used as model protein. The study focuses on the
25 optimization of the grafting conditions to maximize the amount of active protein during the multi-
26 layering process and highlights the impact of the biotinylation ratio of the protein. It is demonstrated
27 that a 3-layer grafting process allows to improve the bulk density of active sites by a 2-fold factor
28 compared to a single layer. This improvement in protein density allows to increase the affinity range
29 of this technique to the millimolar range.

30 **Keywords:** Frontal Affinity Chromatography, Organic monolith, Biofunctionalization, Miniaturization,
31 Nano-liquid Chromatography.

32

33 **1. INTRODUCTION:**

34 Affinity chromatography is widely used in sample preparation to purify and pre-concentrate analytes
35 in complex matrices [1]. This method is furthermore proving to be just as interesting in a niche
36 domain such as the identification/characterization of weak interactions by Weak Affinity
37 Chromatography (WAC).

38 In the latter, the principle is based on the observation of differences in retention between species
39 exhibiting different affinities with targets grafted on the surface of the chromatographic stationary
40 phase. The higher the affinity (i.e. the lower the K_d value), the higher the retention time of a binding
41 ligand [2–5].

42 Weak Affinity Chromatography operated either in zonal or frontal mode has shown to be a powerful
43 and potentially money-saving tool, allowing both the ranking of ligands' affinity [4–6] and the latter
44 determination [7], while reducing resources consumption and analysis time by means of
45 miniaturization [8] and hyphenation with Mass Spectrometry [9,10]. The advantages over other
46 biophysical methods are the ability to analyze complex ligand mixtures such as natural extracts,
47 together with the possibility to re-use the target that is immobilized onto the chromatographic
48 support, thus reducing consumption of targets that can be produced only in minute amounts [11,12].

49 Weak affinity chromatography is suitable for the study of weak affinity interactions (K_d in the range
50 of mM to 0.1 μ M). The identification of ligands of very weak affinity (mM) can be of great interest, for
51 example in the context of Fragment Based Drug Discovery (FBDD) where such weak affinity ligands
52 (also called fragments) are the starting points for the conception of high affinity ligands [13].
53 However, the identification of such starting points can be limited by the amount of active target of
54 interest grafted onto the support. Indeed, for a given K_d value, the retention factor of a ligand is
55 directly related to the bulk density of active target grafted on the support. The weaker the affinity,
56 the higher the required bulk density of active target to detect the affinity i.e. to get a detectable
57 retention. It is therefore of great interest to increase this bulk density in order to extend the
58 detectable affinity range [2,8,14–16].

59 We have recently demonstrated the interest of miniaturizing weak affinity chromatography (using
60 monolithic chromatographic columns in capillary format) to identify weak affinity ligands targeting
61 proteins available in scarce amounts [11]. Targets can be grafted by a traditional direct
62 immobilization (e.g. via aldehyde route) which does not require any protein modification. An
63 alternative approach for the in-situ grafting of such supports is the immobilization of the biotinylated
64 target onto "generic columns" pre-functionalized with streptavidin. The instantaneous and
65 quantitative capture of biotinylated targets by these generic columns makes it possible (i) to
66 immobilize them extemporaneously (a great advantage for targets with low stability), (ii) to reduce

67 the amount of target consumed to what is strictly required thanks to the UV-monitoring of the
68 grafting step [11]. With this approach, we have shown that it is possible to consider fragment
69 screening against membrane proteins embedded in biotinylated biomimetic membranes [7].
70 To extend the reach of WAC and to allow the identification of ligands of ever weaker affinity (a
71 challenge for FBDD), we envisioned to expand on the already adopted streptavidin-biotin interaction
72 and build tridimensional layers of target with the goal of increasing the final number of active sites
73 available. This can be done by employing biotinylated targets with a higher than usual biotin
74 incorporation ratio (>1.5). A first layer of biotinylated target is first immobilized on the streptavidin
75 chromatographic support (Layer 1). At the end of this first step, residual biotin residues are available
76 on the target. A solution of streptavidin is then infused, leading to the capture of an additional layer
77 of streptavidin by the residual biotin residues of the immobilized target (Mid-Layer). Since
78 streptavidin has four active sites, it can capture a next layer of biotinylated target (Layer 2). This
79 layering process can be repeated several times as shown in Figure 1. Biotinylated Concanavalin A was
80 used as target protein model to investigate the impact of multi-layering on affinity chromatography.
81 This protein, belonging to the lectin family, is used in affinity chromatography for its ability to bind
82 molecules containing mannose.

83

84

Figure 1

85 2. MATERIALS AND METHODS

86 2.1. Reagents and chemicals

87 Concanavalin A (ConA) and biotinylated Concanavalin A from *Canavalia ensiformis*, streptavidin (from
88 streptomyces avidinii, affinity purified, $\geq 13 \text{ U mg}^{-1}$ of protein), (3-methacryloxypropyl)-
89 trimethoxysilane (γ -MAPS), ethylene dimethacrylate (EDMA, 97%), glycidyl methacrylate (GMA,
90 98%), 1-propanol, 1,4-butanediol, dimethylsulfoxide (DMSO), sodium periodate, lithium hydroxide,
91 dipotassium hydrogen phosphate (K_2HPO_4), o-phosphoric acid, acetic acid, sodium
92 cyanoborohydride, triethylamine (TEA), Azobisisobutyronitrile (AIBN), p-nitrophenyl- α -D-
93 mannopyranoside were purchased from Sigma Aldrich (L'Isle d'Abeau Chesne, France). All aqueous
94 solutions were prepared using $>18 \text{ M}\Omega$ deionized water. Preparation of the phosphate buffer was
95 done by dissolving 1.17 g of K_2HPO_4 in 100 mL of ultrapure water and pH was adjusted to 7.4 with
96 ortho-phosphoric acid. Thermo Scientific EZ-Link™ NHS-PEG4 Biotinylation Kit from thermo
97 (Thermofischer Scientific, France).

98 2.2. Biochemistry methods:

99 2.2.1. Biotinylated Concanavalin A:

100 Concanavalin A was biotinylated with a long chain (29 Å), water soluble biotinylating reagent using
101 the Thermo Scientific EZ-Link™ NHS-PEG4 Biotinylation Kit, following the manufacturer's instructions.
102 The biotinylation molar excess was varied to control the biotinylation ratio.

103 2.2.2. Biotin incorporation ratio evaluation:

104 The biotin incorporation ratio was estimated thanks to the 4'-hydroxyazobenzene-2-carboxylic acid
105 (HABA) Assay, executed with the reagents included in the Thermo Scientific EZ-Link™ NHS-PEG4
106 Biotinylation Kit.

107 2.3. Instrumentation

108 A microfluidic flow controller MFCS-EZ100 system (Fluigent, Villejuif, France) was used to flow liquids
109 into capillary columns. An LC pump LC 10AD (Shimadzu, Tokyo, Japan) was used to rinse the freshly
110 prepared capillaries.

111 Frontal Weak Affinity Chromatography experiments were carried out with a 7100 capillary
112 electrophoresis Agilent system (Agilent Technologies, Waldbronn, Germany) equipped with a diode
113 array detector and an external nitrogen tank to reach pressures up to 12 bar. System control and
114 data acquisition were carried out using the Chemstation software (Agilent). All experiments were

115 carried out at 25°C in “short-end” injection mode, with the inlet of the capillary immersed in the
116 solution to be infused.

117 **2.4. Capillary monolith synthesis and biofunctionalization**

118 *2.4.1. Poly GMA-co-EDMA monolith synthesis:*

119 Poly(GMA-co-EDMA) monoliths were synthesized inside fused-silica capillaries presenting a UV
120 transparent coating (TSH, 75 µm i.d., Cluzeau Info Labo, France) as already described in previous
121 works [17,18]. Capillaries were pre-treated by flushing them (1 h, 0.5 bar) with a solution composed
122 of 5% (v/v) γ-MAPS and 2.5% (v/v) TEA in methanol/water (95/5, v/v). They were then rinsed with
123 methanol (15 min, 0.5 bar), and finally dried with a nitrogen stream. The polymerization mixture was
124 prepared by adding to 12 mg of AIBN initiator, 0.9 mL GMA, 0.3 mL EDMA, 1.05 mL 1-propanol,
125 0.6 mL butan-1,4-diol and 0.15 mL ultra-pure water. The polymerization mixture was then agitated
126 (15 minutes) and sonicated (15 minutes), to be then used to fill the pre-treated capillaries at a
127 nitrogen pressure of 1bar. To localize the monolith on a specific length of the capillaries, PEEK
128 tubings (380 µm i.d.) were used to mask non-irradiated areas, limiting the monolith length to about
129 10 cm. A Bio-link UV cross-linker (VWR International, France) was used to carry out the
130 photopolymerization under 365 nm UV light for a total energy of 6 J/cm². After polymerization, the
131 column was immediately rinsed with methanol for 1 h, then cut to reach a monolith length of 8.5 cm.

132 *2.4.2. Preparation of streptavidin-functionalized monolithic capillary columns:*

133 Columns were functionalized with streptavidin as described in the work of Lecas et al. [11]. The
134 epoxy groups present on the GMA-co-EDMA monolith were first hydrolyzed into diols by flushing the
135 columns with 1M sulfuric acid (2h, 6.5 bar) and then washing the column with ultra-pure water (1h,
136 6.5 bar). A periodic acid solution at pH 5.5 was then percolated (1h, 6.5bar) to oxidize the diol groups
137 into aldehyde groups, followed by a quick rinse (67 mM phosphate buffer, pH 6, 15 minutes, 6.5 bar).
138 A 1mg/mL streptavidin and 4mg/mL NaBH₃CN solution in 67 mM pH 6 phosphate buffer was then
139 percolated through the column overnight (18 h, 4.5 bar, room temperature). After streptavidin
140 grafting, the column was flushed with a solution of sodium borohydride 2.5mg/mL in phosphate
141 buffer 67 mM pH 8 (2h, 6.5bar), to reduce residual aldehydes. The resulting streptavidin columns
142 were then stored at 4°C.

143 *2.4.3. Immobilization of biotinylated Concanavalin A on streptavidin-functionalized monolithic* 144 *capillary columns:*

145 Dynamic grafting was carried out by infusing a diluted biotinylated ConA solution (concentration in
146 the μM range in phosphate buffer 67mM, pH 7.4) and monitoring it by *in-situ* UV detection, to stop
147 the grafting once completed (column saturated).

148 2.4.4. Multi-layer grafting procedure:

149 Columns presenting a single layer of ConA were dynamically grafted with streptavidin by flowing a
150 solution of streptavidin at a concentration ranging between 5 and 15 μM in phosphate buffer 67 mM,
151 pH 7.4), monitoring the grafting by in-situ UV detection (Mid-layer). The same process was then
152 repeated with the same sample of biotinylated ConA used for the first layer grafting. This layering
153 process was repeated for up to 3 layers of ConA, evaluating the column by frontal affinity
154 chromatography (FAC) at each step, using HABA as test ligand for the streptavidin mid-layers, and p-
155 nitrophenyl- α -D-mannopyranoside for ConA layers.

156 2.5. Frontal affinity chromatography (FAC) experiments

157 FAC was used to determine the amount of ConA active sites ($B_{act,ConA}$) at each layer and mid-layer and
158 the amount of Streptavidin active sites ($B_{act,Strepta}$) at each mid-layer. For the results presented in this
159 manuscript, a variation of FAC addressed as “staircase FAC”[19] (similar to that seen in the work of
160 He et al. [20]) was employed (see S1 for the rationale of the staircase approach). Solutions of
161 increasing concentrations of the test ligand were percolated consecutively in the column (without
162 any rinsing step in-between the percolations of the different concentrations).

163 2.5.1. Determination of the amount of Concanavalin A active sites ($B_{act,ConA}$)

164 P-nitrophenyl- α -D-mannopyranoside was used as a weak affinity test ligand to determine the
165 amount of ConA active sites at each step of the grafting (after each layer of ConA and each mid-layer
166 of Streptavidin). Due to the dependence of ConA activity on the presence of Calcium ions, before any
167 activity evaluation, phosphate buffer 67mM enriched with Ca^{2+} (67 mM K_2HPO_4 , pH 7.4, 100 μM Ca^{2+}
168 was percolated through the column for at least 40 minutes, to ensure the maximal activity of the
169 ConA grafted. Solutions of increasing concentrations (5, 7.5, 10, 15, 20, 40 and 500 μM) of P-
170 nitrophenyl- α -D-mannopyranoside were percolated successively. Rationality of the results was
171 ensured by comparing the obtained K_d value with literature value ($K_d \approx 30\text{-}50 \mu\text{M}$ [21,22]). DMSO
172 was used as dead time marker.

173 2.5.2. Determination of the amount of Streptavidin active sites ($B_{act,Strepta}$)

174 For the determination of the amount of streptavidin active sites available at each mid-layer, HABA (K_d
175 = 100 μM) was used as test solute with increasing concentrations (5, 10, 50, 100 and 200 μM).

176 Rationality of the results was ensured by comparing the obtained K_d (range 90-120 μM) with
177 literature values (100 μM) [23].

178

179 3. RESULTS AND DISCUSSION

180 3.1. Influence of the ConA biotinylation ratio on the number of ConA active sites for a monolayer 181 grafting (layer 1)

182 The ConA biotinylation ratio may impact the amount of resulting Concanavalin active sites.
183 Concanavalin was biotinylated with different molar excesses of biotinylation reagent, leading to
184 different biotinylation ratios addressed as “Low”, “Medium” and “High”, relatively to their biotin
185 incorporation ratio (Table 1).

186

187 Table 1 - Biotinylation incorporation ratios obtained at different biotinylation conditions

188

189 The influence of the biotinylation ratio on the amount of ConA active sites ($B_{act, ConA}$) after a single
190 grafting layer has been evaluated for the three biotinylation ratios. $B_{act, ConA}$ values were determined
191 by Frontal Affinity Chromatography, in the staircase mode (see experimental section and S1) that
192 allows obtaining data related to the quantity of active sites in a column (B_{act}) and the dissociation
193 constant of the ligand (K_d).

194

195

Figure 2

196

197 As illustrated Figure 2, the number of ConA active sites is maximum (around 55 pmol per column i.e
198 6.4 pmol cm^{-1} of monolith i.e. $146 \text{ pmol } \mu\text{L}^{-1}$) for “low” or “medium” biotinylation ratios. An increase
199 in the ConA biotinylation ratio leads to a significant decrease (about 20%) in the number of ConA
200 active sites.

201 Indeed, when the ConA biotinylation ratio increases, the probability that several biotins of the same
202 ConA are engaged with multiple underlying streptavidin sites increases. Such a multi-point anchoring
203 of the biotinylated ConA on the streptavidin layer limits the amount of ConA that can be grafted (one
204 ConA occupies several streptavidin active sites).

205 3.2. Influence of the ConA biotinylation ratio on the number of ConA active sites for a multi- 206 layering grafting

207 The impact of the biotinylation ratio on the number of ConA active sites over a multi-step approach
208 was studied by considering 3 successive layers. The amount of ConA active sites was determined at
209 each step and results are presented in Figure 2. The variation of the amount of ConA active sites ($B_{act, ConA}$)
210 through different layers is not comparable for each biotinylation ratio.

211 For the « low » biotinylation ratio, the multi-step approach does not significantly increase the
212 amount of ConA active sites. Indeed, if a gain of about 30% is observed at the end of the second step,
213 a third one doesn't increase the quantity of active sites anymore. After the second grafting cycle
214 (layer 2) , it seems that no free and accessible biotin residue is available on ConA to bind a new
215 streptavidin mid-layer necessary to initiate a third layer of ConA.

216 The behavior is different for the two higher biotinylation rates. Indeed, the amount of ConA active
217 sites increases during the three successive grafting steps.

218 The best grafting outcome (two-fold increase) was observed for the medium biotin incorporation
219 level sample. A medium biotin incorporation ratio is the best compromise to get a first layer with a
220 high ConA density, while making possible to build several layers.

221 To better understand the layering process, the amount of ConA active sites was determined at each
222 layer and mid-layer (Fig 3 up, in green) in order to highlight a potential deactivation of the already
223 grafted ConA (reduction of the number of active sites) consecutive to the addition of a new
224 streptavidin mid-layer. At the same time, the amount of streptavidin active sites ($B_{act,Strepta}$) added at
225 each mid-layer was also evaluated (Figure 3, bottom, in blue).

226 It can be observed that the 1st streptavidin mid-layer deactivates part of the previously grafted ConA.
227 The higher the degree of biotinylation of ConA, the stronger this partial deactivation (10 % for the
228 “medium” biotinylation rate and more than 50 % for the “high” one). This loss of activity may be due
229 to a decrease in accessibility to ConA due to the grafting of the streptavidin mid- layer. Indeed, the
230 loss ConA active sites is higher for greater amounts of streptavidin added at the mid-layer (loss of
231 10 % and 50 % for amounts of added streptavidin actives sites of 22 pmol and 42 pmol respectively).
232 However, regardless of the extent of this loss of activity, the total amount of active ConA after the
233 second grafting step (layer 2) is greater than that obtained after the first layer.

234

235

Figure 3

236

237 The same trend is observed during the third grafting step *viz* partial deactivation of the grafted ConA
238 following the addition of streptavidin (2d middle-step) and overcompensation of the total amount of
239 ConA active sites by the final ConA grafting step. The best compromise is obtained with the medium
240 biotinylation rate, which limits the deactivation effect while allowing for further grafting of a
241 consistent amount of active ConA at each step.

242 With a medium biotinylation ratio, a 3-layer grafting process allows to improve the active protein
243 grafting density by a 2-fold factor compared to a single layer. It is worth noticing that such a multi-
244 layering process is automatically implemented, the successive protein solutions being infused with
245 the pressurization system of the capillary electrophoresis device. The overall duration time of a

246 three-layer process is about 3h (30 min for a monolayer). Although it is possible to make more layers,
247 we have estimated that a 3-layer process was the best compromise between the number of active
248 sites and grafting duration. This improvement in bulk density of active sites should allow to increase
249 the affinity range that can be addressed by this technique.

250 **3.3. Detection of very weak affinity**

251 As stated earlier in the text, frontal weak affinity chromatography is useful to identify very weak
252 affinity ligands in early stages of drug discovery processes. For a compound with no affinity for the
253 immobilized target, the breakthrough time t_p measured is independent of the concentration of the
254 infused ligand. ($t_p = t_0$ if no non-specific interactions occur and $t_p > t_0$ in the case of non-specific
255 interactions). For a compound with affinity for the target, the breakthrough time depends on the
256 ligand concentration that is infused. The ability to detect weak affinity ligands in FAC is based on the
257 shift in breakthrough times Δt_p that can be non-equivocally detected between two extremely
258 different ligand concentrations (concentrations of about 0,1Kd and 10Kd). For comparison purposes,
259 this difference in plateau time Δt_p must be normalized by dividing it by the dead time and can be
260 then expressed as $\Delta t_p/t_0$.

261 The reduced breakthrough time difference $\Delta t_p/t_0$ is directly correlated to both the strength of the
262 affinity interaction and the quantity of protein target interacting in the column. Increasing the
263 quantity of protein target available for the interaction in the column consequently allows to detect
264 weaker interactions (higher Kd).

265 To illustrate the improvement regarding the extension of the detectable affinity range by the
266 proposed grafting strategy, a weaker affinity ligand (p-nitrophenyl- α -D-glucopyranoside Kd > 200 μ M
267 [22,24]), was used as test ligand.

268 Figure 4 shows the frontal affinity chromatograms obtained for two different concentrations (10 μ M
269 and 2000 μ M) of p-nitrophenyl- α -D-glucopyranoside for a single-layer ($B_{act} = 52.4 \pm 0.5$ pmol) and on
270 a 3-layers ConA column ($B_{act} = 95 \pm 0.7$ pmol). The plot shows how the difference in breakthrough
271 time difference changes greatly due to the number of ConA active sites increase due to the layering
272 strategy.

273

274

274 **Figure 4**

275

276 Empirically, the limit of affinity detection (the minimum value of $\Delta t_p/t_0$ needed to be able to
277 confidently recognize specific affinity) was evaluated to be 0.1 . Considering the gain in the amount
278 of active protein on the column (about 2-fold), the affinity range is extended allowing the detection

279 of lower affinity. The lowest affinity observable with the resulting Bact values can be estimated being
280 in the range of 1mM in Kd.

281 **4. CONCLUSIONS**

282 A novel approach to increase the amount of active protein that can be immobilized on organic
283 monolithic capillary column was presented. This approach implements a multi-step process of
284 protein immobilization based on the streptavidin-biotin interaction and involves the use of multi-
285 biotinylated proteins. Biotinylation of proteins is quite easily done and controlled using a commercial
286 biotinylation reagent kit. The streptavidin-biotin interaction is fast and quantitative allowing to
287 prepare multi-layers without any loss of protein sample and for a limited increase in preparation
288 time. However, this straightforward approach requires to carefully control the number of biotin
289 molecules borne by proteins, to be efficient. Whereas a low biotinylation ratio i.e. < 2 is optimal to
290 prepare dense monolayers using a single grafting step, a higher biotinylation ratio (higher than 2) is
291 required for the multilayering approach. The most interesting biotinylation rate for a multi-step
292 approach is the intermediate one. Compared to a single layer, optimal grafting condition allows twice
293 the density while doubling retention properties and extending the affinity range.

294 This approach is simple and can easily be applied to other biomolecules that can be biotinylated
295 and/or to other methods requiring the preparation of a biofunctionalized layer (e.g biosensors,
296 microfluidic lab-on-chips).

297 **Declaration of Competing Interest**

298 The authors declare that they have no known competing financial interest or personal relationships
299 that could have appeared to influence the work reported in this paper.

300 **Acknowledgement**

301 This work was supported by the Institut de Recherche Servier IDRS (France). We thank Ian Ramtanon
302 for his final english proof reading.

- 304 [1] W.-C. Lee, K.H. Lee, Applications of affinity chromatography in proteomics, *Anal. Biochem.* 324
305 (2004) 1–10. <https://doi.org/10.1016/j.ab.2003.08.031>.
- 306 [2] F. Tsopelas, A. Tsantili-Kakoulidou, Advances with weak affinity chromatography for fragment
307 screening, *Expert Opin. Drug Discov.* 14 (2019) 1125–1135.
308 <https://doi.org/10.1080/17460441.2019.1648425>.
- 309 [3] S. Ohlson, M.-D. Duong-Thi, Weak Affinity Chromatography (WAC), in: 2017: pp. 107–130.
310 <https://doi.org/10.1002/9781119099512.ch7>.
- 311 [4] M.-D. Duong-Thi, E. Meiby, M. Bergström, T. Fex, R. Isaksson, S. Ohlson, Weak affinity
312 chromatography as a new approach for fragment screening in drug discovery, *Anal. Biochem.*
313 414 (2011) 138–146. <https://doi.org/10.1016/j.ab.2011.02.022>.
- 314 [5] D.S. Hage, Analysis of Biological Interactions by Affinity Chromatography: Clinical and
315 Pharmaceutical Applications, *Clin. Chem.* 63 (2017) 1083–1093.
316 <https://doi.org/10.1373/clinchem.2016.262253>.
- 317 [6] E. Meiby, H. Simmonite, L. le Strat, B. Davis, N. Matassova, J.D. Moore, M. Mrosek, J. Murray,
318 R.E. Hubbard, S. Ohlson, Fragment Screening by Weak Affinity Chromatography: Comparison
319 with Established Techniques for Screening against HSP90, (2013).
320 <https://doi.org/10.1021/ac400715t>.
- 321 [7] L. Lecas, L. Hartmann, L. Caro, S. Mohamed-Bouteben, C. Raingeval, I. Krimm, R. Wagner, V.
322 Dugas, C. Demesmay, Miniaturized weak affinity chromatography for ligand identification of
323 nanodiscs-embedded G-protein coupled receptors, *Anal. Chim. Acta.* 1113 (2020).
324 <https://doi.org/10.1016/j.aca.2020.03.062>.
- 325 [8] X. Zheng, Z. Li, S. Beeram, M. Podariu, R. Matsuda, E.L. Pfaunmiller, C.J.W. li, N. Carter, D.S.
326 Hage, Analysis of biomolecular interactions using affinity microcolumns: A review, *J.*
327 *Chromatogr. B.* 968 (2014) 49–63. <https://doi.org/10.1016/j.jchromb.2014.01.026>.
- 328 [9] S. Ohlson, M.-D. Duong-Thi, Fragment screening for drug leads by weak affinity
329 chromatography (WAC-MS), *Methods.* 146 (2018) 26–38.
330 <https://doi.org/10.1016/j.ymeth.2018.01.011>.
- 331 [10] M.C. de Moraes, C. Temporini, E. Calleri, G. Bruni, R.G. Ducati, D.S. Santos, C.L. Cardoso, Q.B.
332 Cass, G. Massolini, Evaluation of capillary chromatographic supports for immobilized human
333 purine nucleoside phosphorylase in frontal affinity chromatography studies, *J. Chromatogr. A.*
334 1338 (2014) 77–84. <https://doi.org/10.1016/j.chroma.2014.02.057>.
- 335 [11] L. Lecas, J. Randon, A. Berthod, V. Dugas, C. Demesmay, Monolith weak affinity
336 chromatography for μ g-protein-ligand interaction study, *J. Pharm. Biomed. Anal.* 166 (2019).
337 <https://doi.org/10.1016/j.jpba.2019.01.012>.
- 338 [12] M.-D. Duong-Thi, G. Bergström, C.-F. Mandenius, M. Bergström, T. Fex, S. Ohlson, Comparison
339 of weak affinity chromatography and surface plasmon resonance in determining affinity of
340 small molecules, *Anal. Biochem.* 461 (2014) 57–59. <https://doi.org/10.1016/j.ab.2014.05.023>.
- 341 [13] P.J. Hajduk, J. Greer, A decade of fragment-based drug design: strategic advances and lessons
342 learned, *Nat. Rev. Drug Discov.* 6 (2007) 211–219. <https://doi.org/10.1038/nrd2220>.
- 343 [14] K. Kasai, Frontal affinity chromatography: An excellent method of analyzing weak biomolecular
344 interactions based on a unique principle, *Biochim. Biophys. Acta BBA - Gen. Subj.* 1865 (2021)
345 129761. <https://doi.org/10.1016/j.bbagen.2020.129761>.
- 346 [15] L. Lecas, V. Dugas, C. Demesmay, Affinity Chromatography: A Powerful Tool in Drug Discovery
347 for Investigating Ligand/membrane Protein Interactions, *Sep. Purif. Rev.* (2020) 1–18.
348 <https://doi.org/10.1080/15422119.2020.1749852>.
- 349 [16] X. Zheng, M. Podariu, C. Bi, D.S. Hage, Development of enhanced capacity affinity
350 microcolumns by using a hybrid of protein cross-linking/modification and immobilization, *J.*
351 *Chromatogr. A.* 1400 (2015) 82–90. <https://doi.org/10.1016/j.chroma.2015.04.051>.

- 352 [17] A. Bruchet, V. Dugas, C. Mariet, F. Goutelard, J. Randon, Improved chromatographic
353 performances of glycidyl methacrylate anion-exchange monolith for fast nano-ion exchange
354 chromatography, *J. Sep. Sci.* 34 (2011) 2079–2087. <https://doi.org/10.1002/jssc.201100180>.
- 355 [18] C. Faye, J. Chamieh, T. Moreau, F. Granier, K. Faure, V. Dugas, C. Demesmay, O. Vandennee-
356 Trambouze, In situ characterization of antibody grafting on porous monolithic supports, *Anal.*
357 *Biochem.* 420 (2012) 147–154. <https://doi.org/10.1016/j.ab.2011.09.016>.
- 358 [19] C. Temporini, G. Massolini, G. Marucci, C. Lambertucci, M. Buccioni, R. Volpini, E. Calleri,
359 Development of new chromatographic tools based on A2A adenosine receptor subtype for
360 ligand characterization and screening by FAC-MS, *Anal. Bioanal. Chem.* 405 (2013) 837–845.
361 <https://doi.org/10.1007/s00216-012-6353-4>.
- 362 [20] X. He, Y. Sui, S. Wang, Stepwise frontal affinity chromatography model for drug and protein
363 interaction, *Anal. Bioanal. Chem.* 410 (2018) 5807–5815. [https://doi.org/10.1007/s00216-018-](https://doi.org/10.1007/s00216-018-1194-4)
364 [1194-4](https://doi.org/10.1007/s00216-018-1194-4).
- 365 [21] R.D. Gray, R.H. Glew, The kinetics of carbohydrate binding to concanavalin A, *J. Biol. Chem.* 248
366 (1973) 7547–7551.
- 367 [22] R.D. Farina, R.G. Wilkins, Kinetics of interaction of some alpha- and beta-D-monosaccharides
368 with concanavalin A, *Biochim. Biophys. Acta.* 631 (1980) 428–438.
369 [https://doi.org/10.1016/0304-4165\(80\)90019-7](https://doi.org/10.1016/0304-4165(80)90019-7).
- 370 [23] S. Repo, T.A. Paldanius, V.P. Hytönen, T.K.M. Nyholm, K.K. Halling, J. Huuskonen, O.T.
371 Pentikäinen, K. Rissanen, J.P. Slotte, T.T. Airene, T.A. Salminen, M.S. Kulomaa, M.S. Johnson,
372 Binding Properties of HABA-Type Azo Derivatives to Avidin and Avidin-Related Protein 4, *Chem.*
373 *Biol.* 13 (2006) 1029–1039. <https://doi.org/10.1016/j.chembiol.2006.08.006>.
- 374 [24] Y. Oda, K. Kasai, S. Ishii, Studies on the Specific Interaction of Concanavalin A and Saccharides
375 by Affinity Chromatography. Application of Quantitative Affinity Chromatography to a
376 Multivalent System, *J. Biochem. (Tokyo)*. 89 (1981) 285–296.
377 <https://doi.org/10.1093/oxfordjournals.jbchem.a133192>.
- 378

379 **Figure captions**

380 **Figure 1:**

381 Schematic illustration of the immobilization process through streptavidin-biotin multi-layering.

382 **Figure 2:**

383 Effect of different biotinylation ratios on $B_{act,ConA}$ by multilayering approach ($B_{act,ConA}$ evaluated after
384 each layering step) ($n \geq 3$).

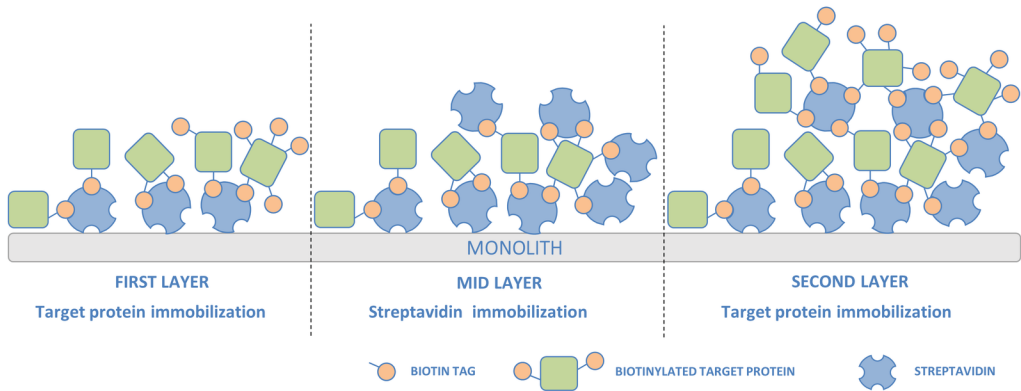
385 **Figure 3:**

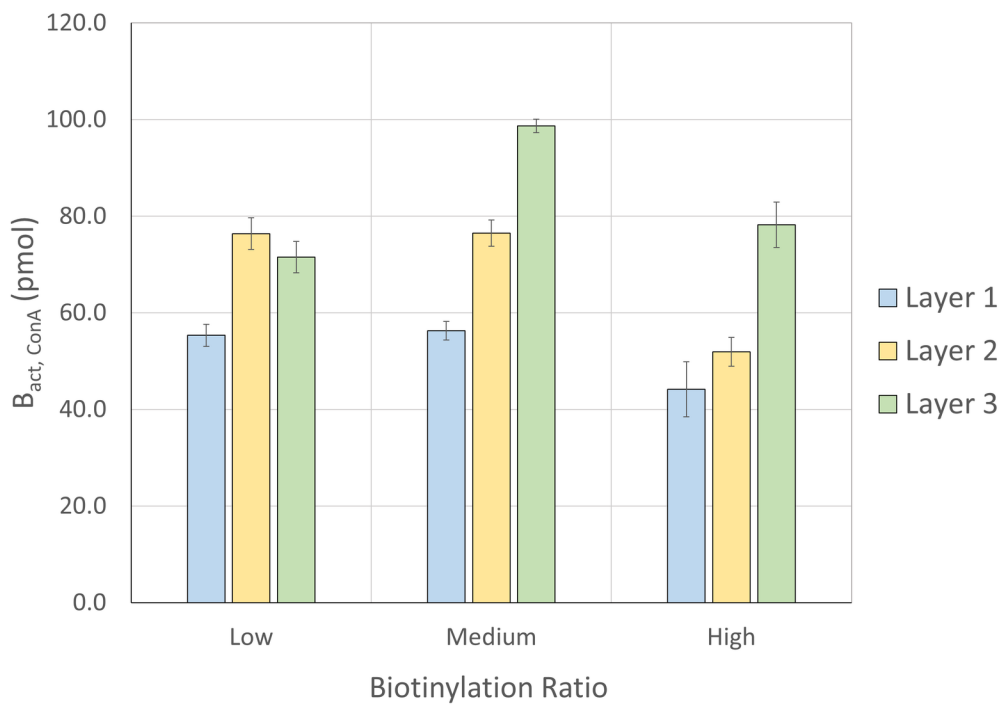
386 Plot representing the evolution of the number of ConA active sites ($B_{act, ConA}$) and the quantity of
387 streptavidin ($B_{act,Strepta}$) added on monolithic columns at each step of the 3-step grafting process
388 using Medium and High biotinylation ratios.(light color for a medium biotinylation ratio and dark
389 color for a high one)

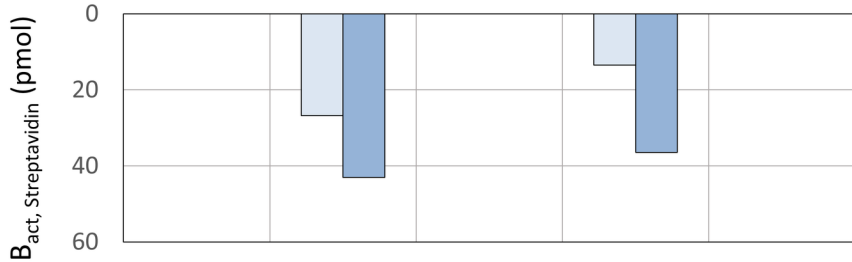
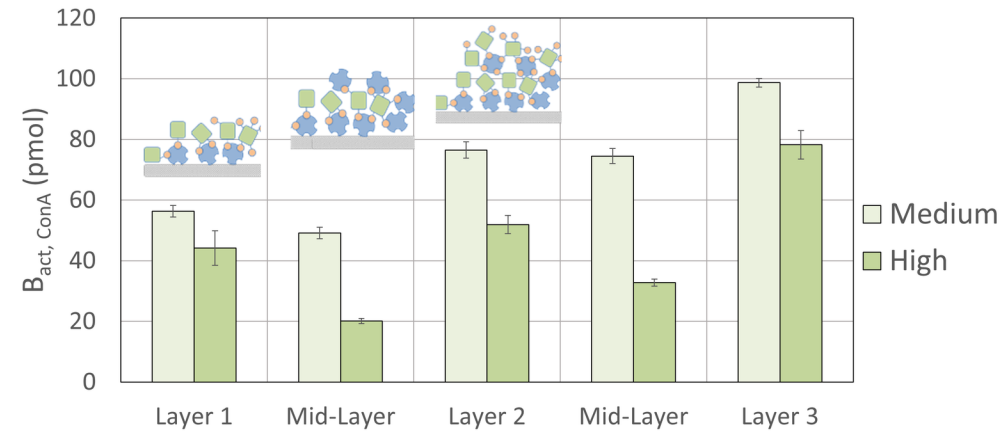
390 **Figure 4:**

391 Frontal affinity chromatograms of p-nitrophenyl- α -D-glucopyranoside at two concentrations,
392 obtained for a column grafted with a single layer of ConA (solid line) and a column grafted with 3
393 layers of ConA (dotted line) using a medium biotin incorporation level.

394







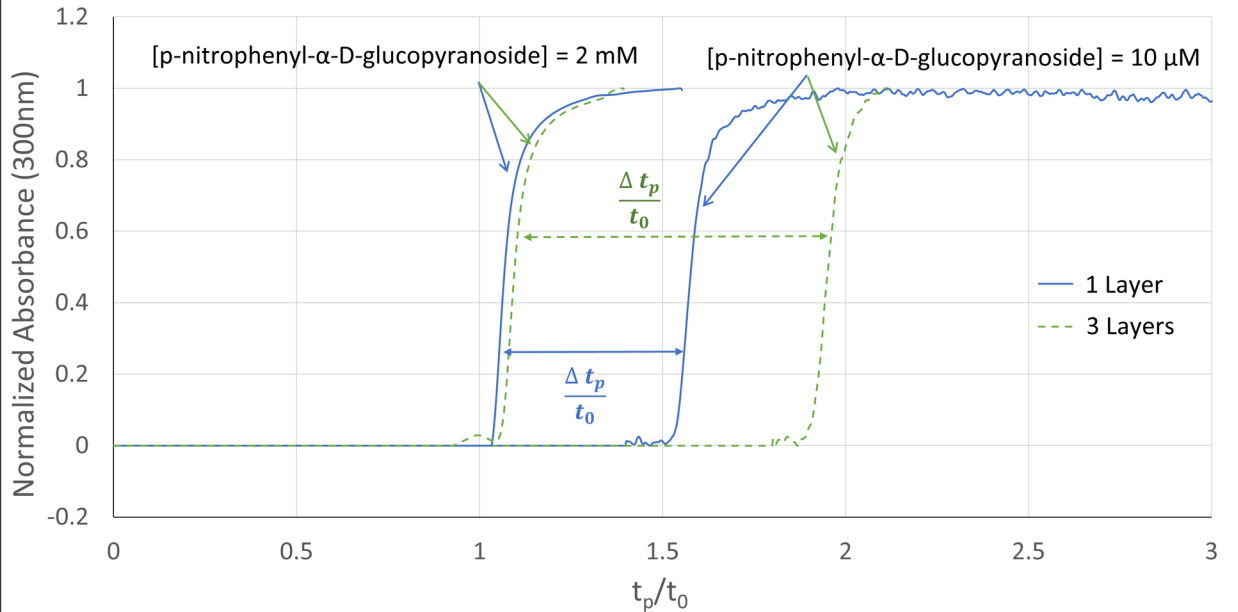


Table 1 - Biotinylation incorporation ratios obtained at different biotinylation conditions

| <i>Sample name</i> | <i>Biot. molar excess</i> | <i>Mean Biot. inc. ratio</i> | <i>Std (n = 5)</i> |
|---------------------------|----------------------------------|-------------------------------------|---------------------------|
| Low | 10x | 1.9 | ± 0.4 |
| Medium | 15x | 2.8 | ± 0.7 |
| High | Commercial sample | 7.5 | ± 0.9 |